

Supporting Information

Fe₃N Decorated Porous Carbon Frameworks from Wheat Flour with Dual Enzyme-mimicking Activities for Organic Pollutants Degradation

Qi Fang,^{a,b} Quanyi Liu,^{a,b} Yu Zhang^{a,b} and Yan Du^{*a,b}

^a State Key Laboratory of Electroanalytical Chemistry, Changchun Institute of Applied Chemistry, Chinese Academy of Sciences, Changchun, Jilin 130022, P. R. China

^b School of Applied Chemistry and Engineering, University of Science & Technology of China, Hefei, Anhui 230026, China

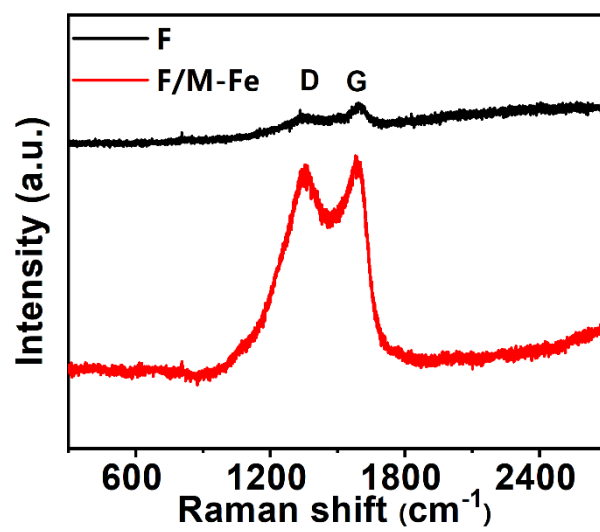


Figure S1. Raman spectra of F and F/M-Fe.

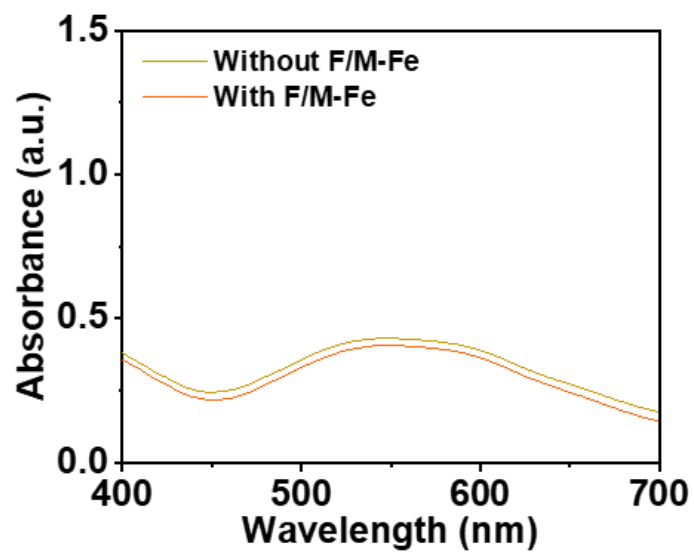


Figure S2. SOD-like activity assay of F/M-Fe using NBT probe as indicator.

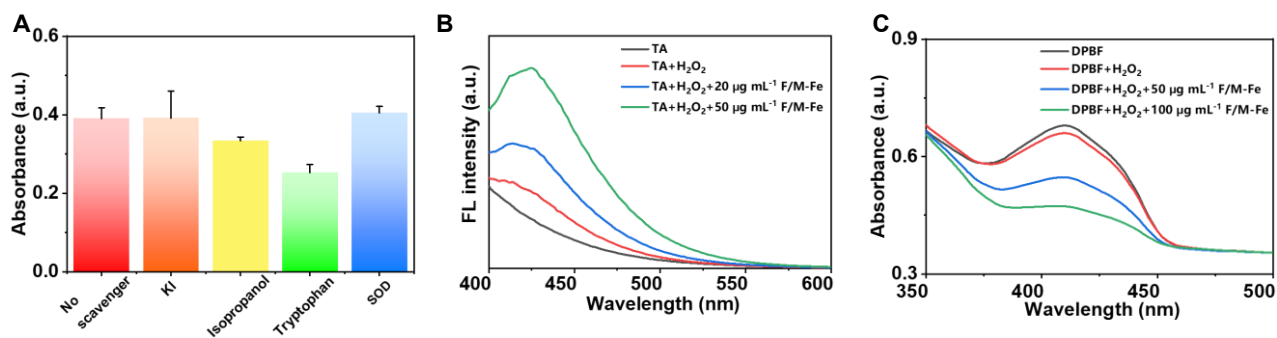


Figure S3. (A) Effect of different scavengers on the catalytic oxidation of TMB by F/M-Fe. (B) Fluorescence spectra of produced hydroxyl radicals ($\cdot\text{OH}$) by using TA assay. (C) UV-Vis absorption spectra of produced singlet oxygen ($^1\text{O}_2$) by using DPBF assay.

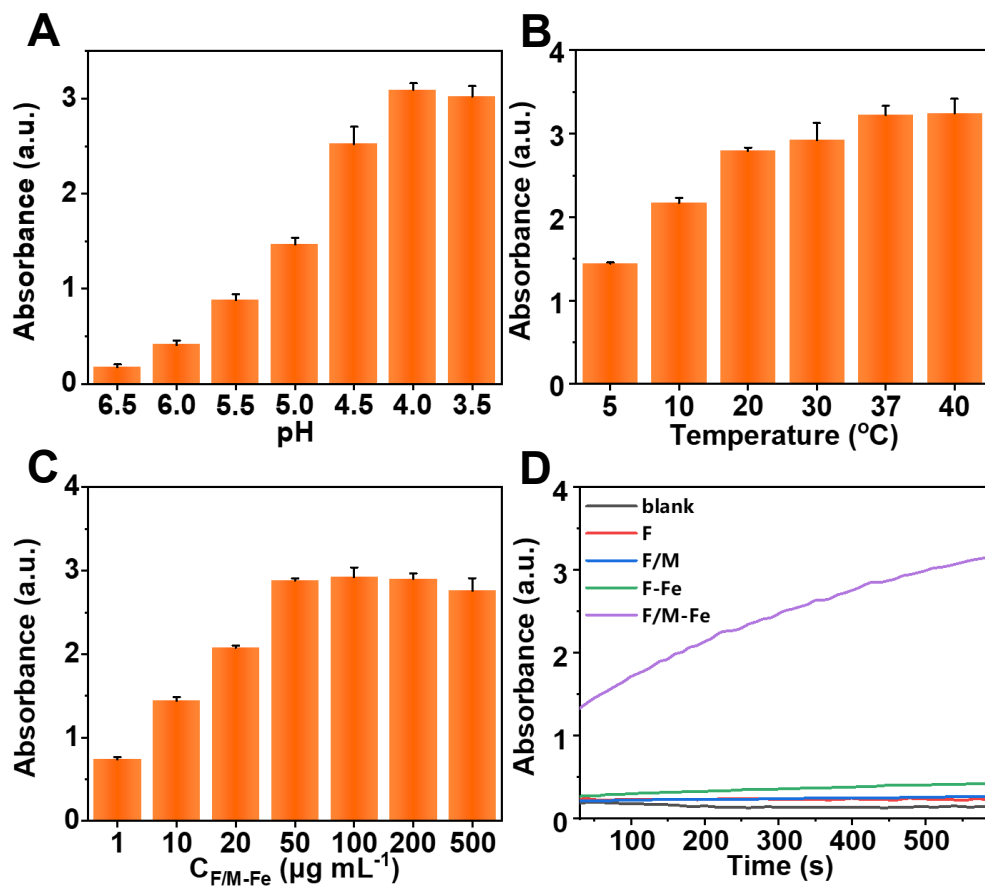


Figure S4. The optimization for (A) pH, (B) temperature and (C) the concentration of F/M-Fe. (D) Time-dependent absorbance of TMB at 652 nm with carbon-based nanozymes.

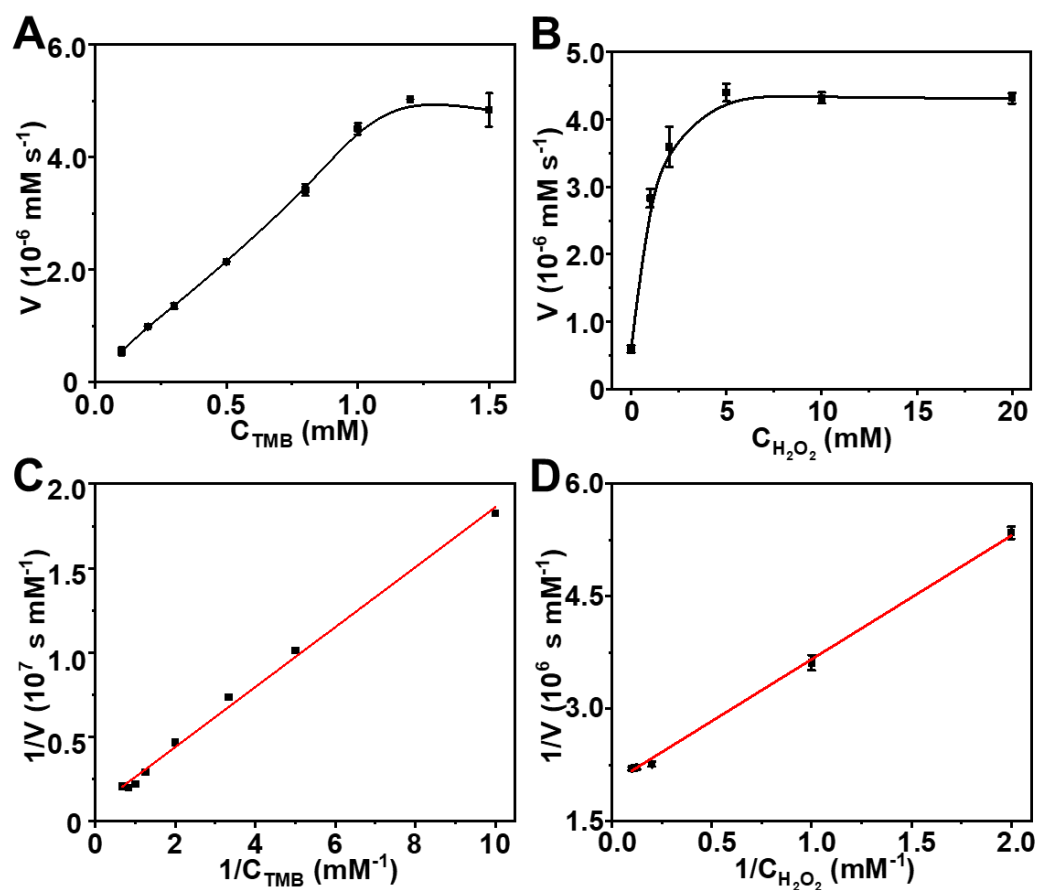


Figure S5. Steady-state kinetic study of the reaction between TMB and H₂O₂ catalyzed by F/M-Fe. The well-fitted Michaelis-Menten curve while varying the concentrations of (A) TMB (0.1, 0.2, 0.3, 0.5, 0.8, 1, 1.2, 1.5 mM) and (B) H₂O₂ (0, 0.5, 1, 2, 5, 8, 10, 20 mM). (C-D) The double reciprocal plots obtained from (A) and (B).

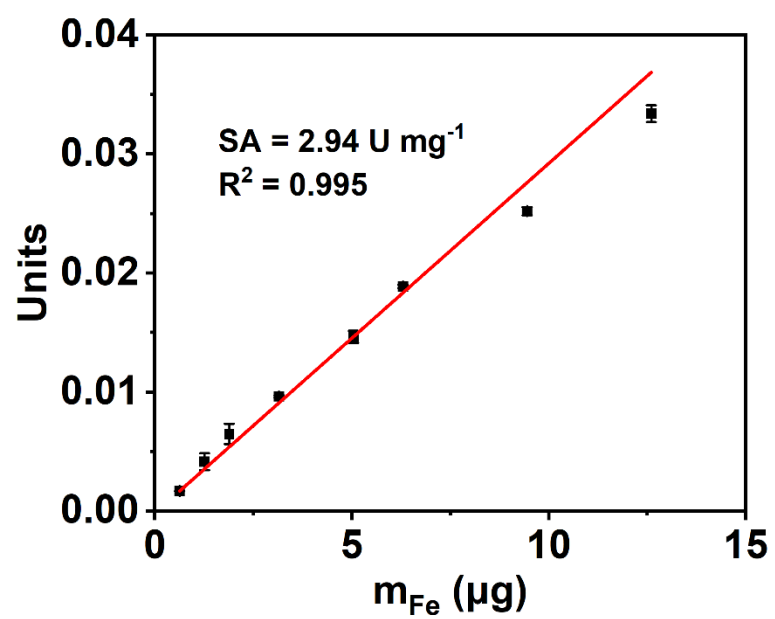


Figure S6. The specific activity value of F/M-Fe. m_{Fe} is mass of Fe in F/M-Fe.

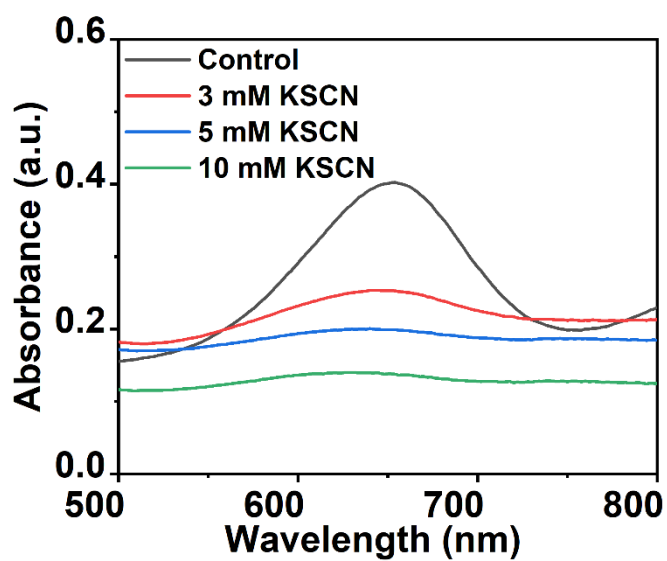


Figure S7. UV-vis absorption spectra of $\text{H}_2\text{O}_2/\text{TMB}/\text{F/M-Fe}$ solution upon the addition of various concentrations of KSCN.

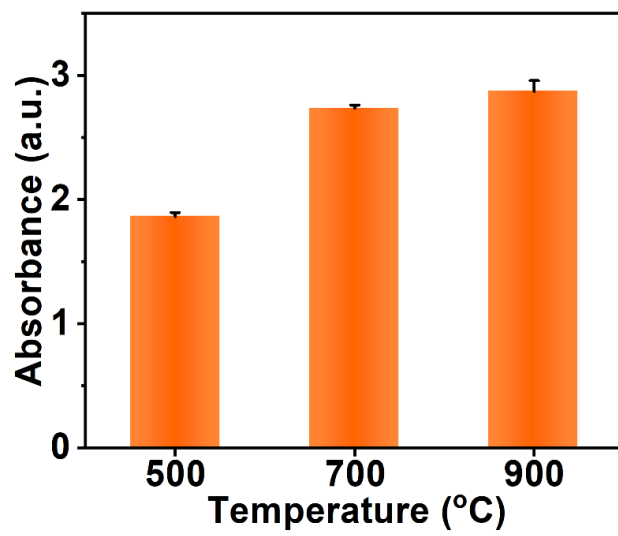


Figure S8. Optimization of the calcination temperature during pyrolysis.

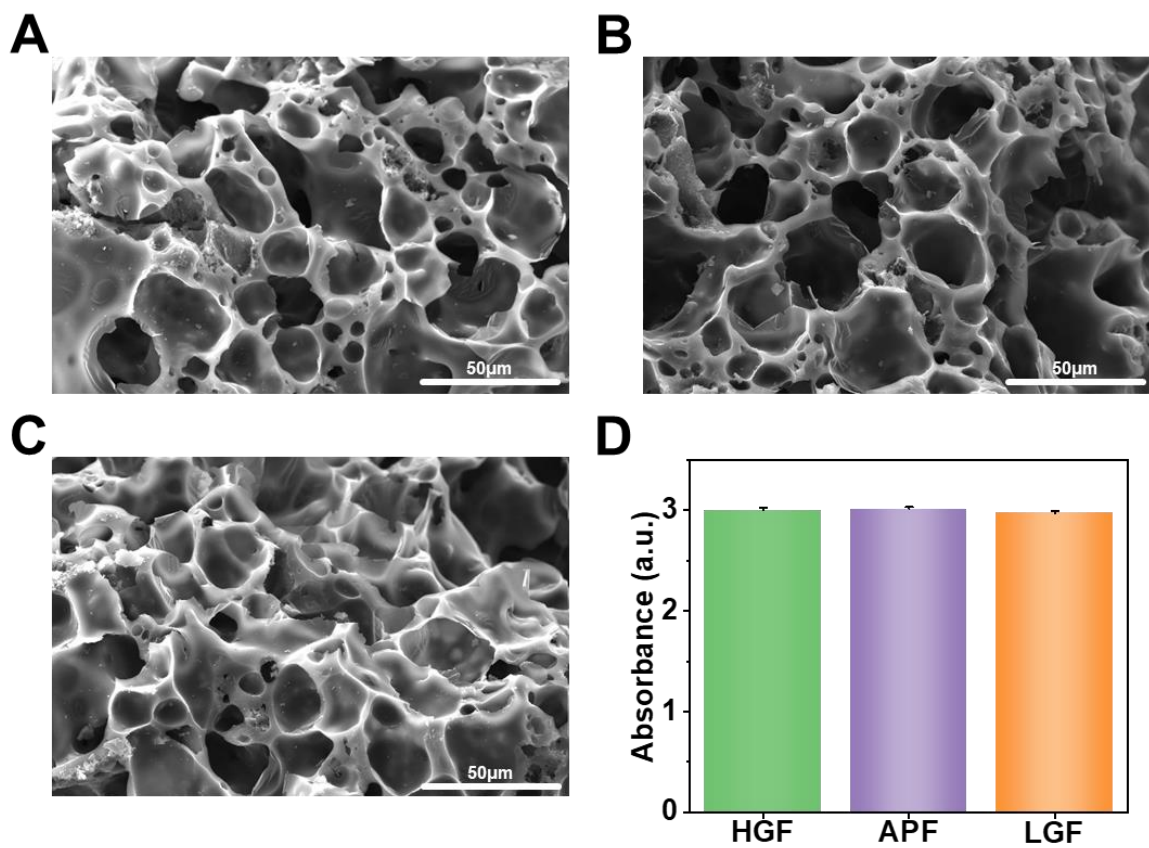


Figure S9. The SEM images of F/M-Fe with different types of wheat flour as precursors: (A) high-gluten flour (HGF); (B) all-purpose flour (APF); (C) low-gluten flour (LGF), and (D) the comparison for the respective peroxidase-like activity of each sample.

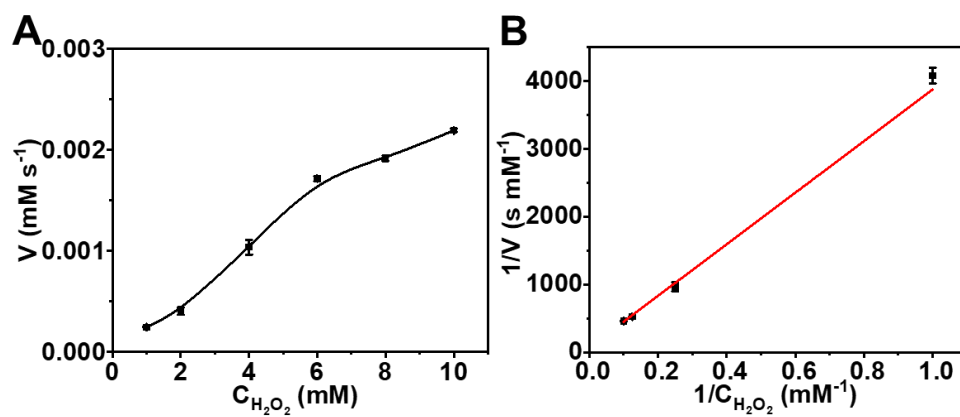


Figure S10. (A) Michaelis-Menten curve fit and (B) Lineweaver-Burk double reciprocal plot of CAT-like activity of F/M-Fe.

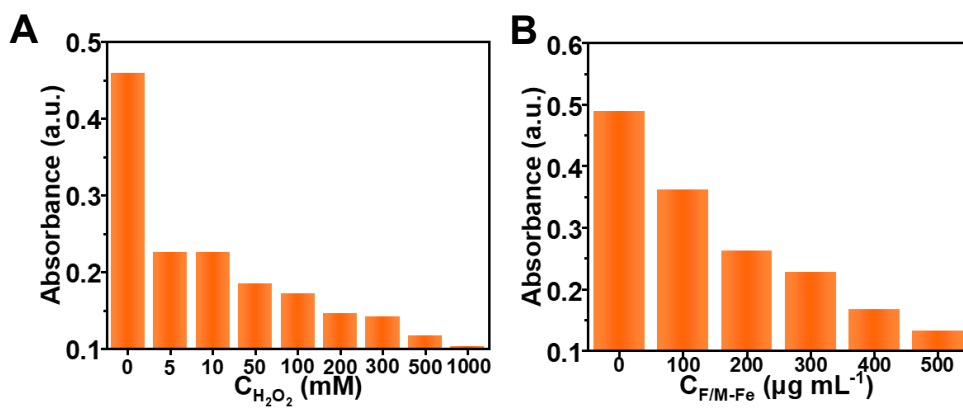


Figure S11. Optimization for the concentration of H₂O₂ (A) and F/M-Fe (B) for MB degradation.

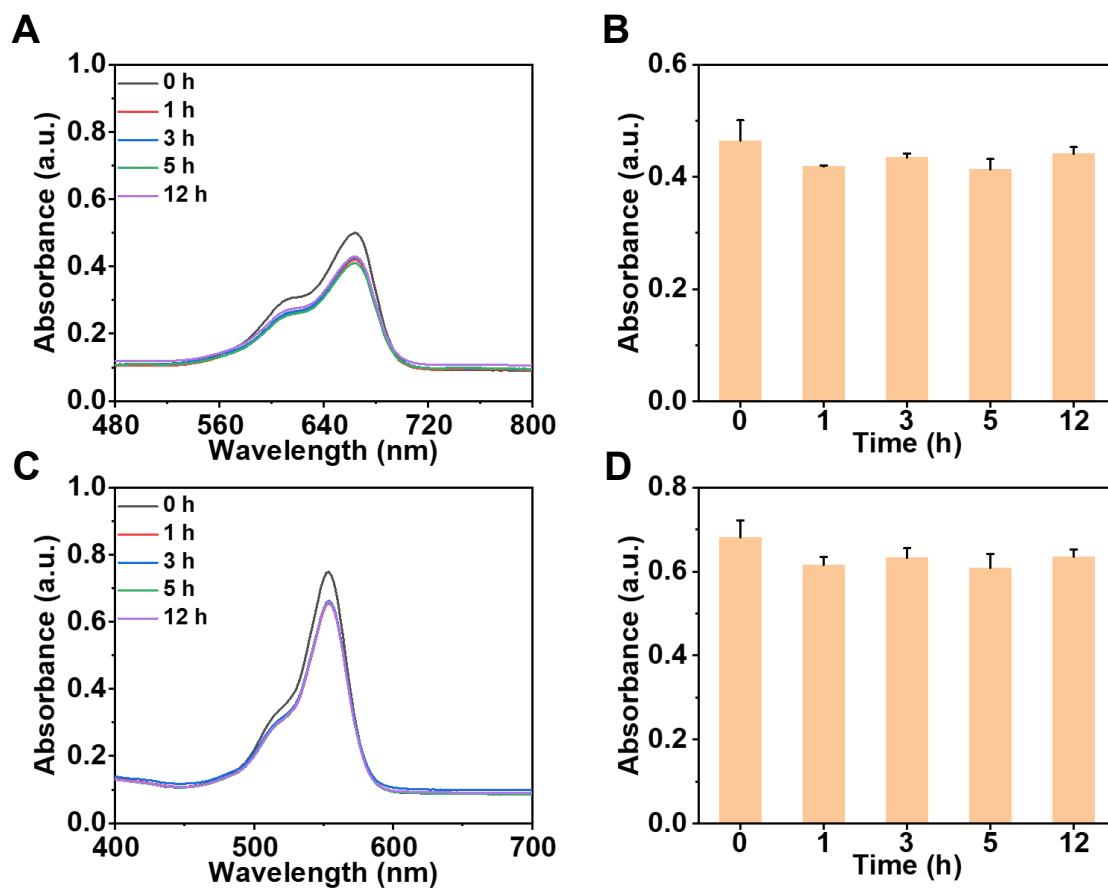


Figure S12. (A) UV-vis absorption spectra of MB subjected to F/M-Fe with different incubation time; (B) Comparison of the absorbance at 664 nm of MB; (C) UV-vis absorption spectra of RhB subjected to F/M-Fe with different incubation time; (D) Comparison of the absorbance at 550 nm of RhB.

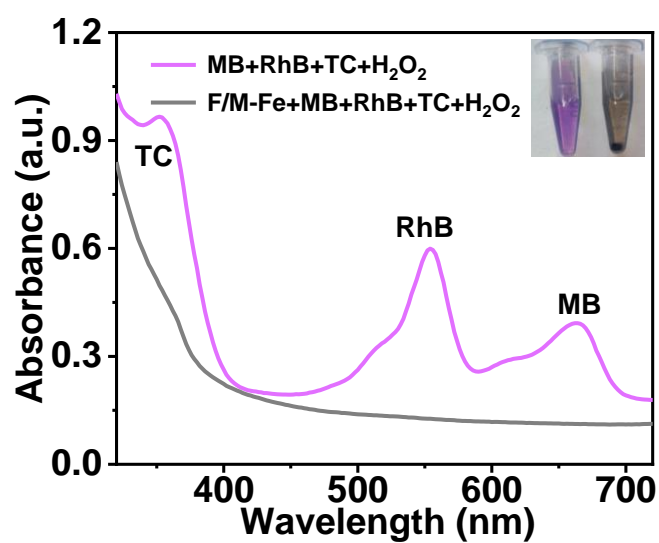


Figure S13. UV-Vis spectra of the pollutant mixture solution (10 μM MB + 10 μM RhB + 0.05 mg mL^{-1} TC) before and after degradation with F/M-Fe in the presence of 1 M H_2O_2 . (The inset picture is the color change of mixture solution before and after degradation)

Table S1. Comparison of kinetic parameters (POD) of F/M-Fe, HRP and other carbon-based enzyme mimics.

| | Substance | K_m (mM) | V_{max} (10^{-8} mM/s) | Reference |
|--|-------------------------------|------------|-----------------------------|-----------|
| F/M-Fe | TMB | 2.07 | 113 | This work |
| | H ₂ O ₂ | 0.82 | 49.7 | |
| HRP | TMB | 0.434 | 10 | 1 |
| | H ₂ O ₂ | 3.7 | 8.71 | |
| GO-COOH | TMB | 0.0237 | 3.45 | 2 |
| | H ₂ O ₂ | 3.99 | 3.85 | |
| CQDs | TMB | 0.039 | 3.61 | 3 |
| | H ₂ O ₂ | 26.77 | 3.06 | |
| GQDs | H ₂ O ₂ | 0.49 | 2.62 | 4 |
| Carbon nanohorn | H ₂ O ₂ | 49.8 | 2.07 | 5 |
| C ₆₀ [C(COOH) ₂] ₂ | H ₂ O ₂ | 24.58 | 4.01 | 6 |

Table S2. Comparison for the kinetic parameters (CAT) of F/M-Fe, catalase and other enzyme mimics.

| | K_m (mM) | V_{max} (mM/min) | Reference |
|---------------------------|------------|--------------------|-----------|
| F/M-Fe | 54.4 | 0.87 | This work |
| Catalase | 294.4 | 0.18 | 7 |
| Fe ³⁺ /AMP CPs | 112.2 | 0.144 | |
| DMSN@AuPtCo | 5.9 | 0.34 | 8 |
| L-QDs | 432.7 | 0.08 | 9 |
| Fe-SANzyme | 18.8 | 0.559 | 10 |
| PCNSs | 678.9 | 0.007 | 11 |

Table S3. Comparison of different catalysts in previous studies and this study.

| Catalyst | Reaction condition | Substrate | Degradation efficiency | Time (h) | Reference |
|--|---------------------------|-----------|------------------------|----------|-----------|
| F/M-Fe | \ | MB | 99.72% | 1 | This work |
| | | RhB | 93.43% | 1 | |
| | | TC | 82.01% | 1 | |
| V ₂ O ₅ /g-C ₃ N ₄ | Visible light irradiation | RhB | 95.5% | 1 | 12 |
| | | TC | 75.7% | 2 | |
| CuCr ₂ O ₄ /CeO ₂ | \ | MB | 99% | 0.75 | 13 |
| | | RhB | 85% | 0.75 | |
| Bi ₂ WO ₆ /Nb ₂ CT _x | Visible light irradiation | MB | 92.7% | 1.5 | 14 |
| | | RhB | 99.8% | 1.5 | |
| | | TC | 83.1% | 2 | |
| ZnO ₂ /Fe ³⁺ | \ | TC | 90% | 1 | 15 |
| GOQD-MPS | \ | RhB | 92% | 6 | 16 |

Reference

1. L. Gao, J. Zhuang, L. Nie, J. Zhang, Y. Zhang, N. Gu, T. Wang, J. Feng, D. Yang, S. Perrett and X. Yan, *Nat. Nanotechnol.*, 2007, **2**, 577-583.
2. Y. J. Song, K. G. Qu, C. Zhao, J. S. Ren and X. G. Qu, *Adv. Mater.*, 2010, **22**, 2206-2210.
3. W. B. Shi, Q. L. Wang, Y. J. Long, Z. L. Cheng, S. H. Chen, H. Z. Zheng and Y. M. Huang, *Chem. Commun.*, 2011, **47**, 6695-6697.
4. Y. Zhang, C. Y. Wu, X. J. Zhou, X. C. Wu, Y. Q. Yang, H. X. Wu, S. W. Guo and J. Y. Zhang, *Nanoscale*, 2013, **5**, 1816-1819.
5. E. L. G. Samuel, D. C. Marcano, V. Berka, B. R. Bitner, G. Wu, A. Potter, R. H. Fabian, R. G. Pautler, T. A. Kent, A. L. Tsai and J. M. Tour, *Proc. Natl. Acad. Sci. U. S. A.*, 2015, **112**, 2343-2348.
6. R. Li, M. Zhen, M. Guan, D. Chen, G. Zhang, J. Ge, P. Gong, C. Wang and C. Shu, *Biosens Bioelectron*, 2013, **47**, 502-507.
7. M. Z. Jiao, Z. J. Li, X. L. Li, Z. J. Zhang, Q. P. Yuan, F. Vriesekoop, H. Liang and J. W. Liu, *Chem. Eng. J.*, 2020, **388**, 9.
8. F. M. Wang, Y. Zhang, Z. W. Liu, J. S. Ren and X. G. Qu, *Nanoscale*, 2020, **12**, 14465-14471.
9. Q. F. Li, Y. L. Gao, J. Shen, X. Y. Mu, J. Y. Wang, L. F. Ouyang, K. Chen, H. He, J. H. Pei, Q. J. Ren, S. Sun, H. L. Liu, L. Zhou, Y. M. Sun, W. Long, J. N. Zhang and X. D. Zhang, *Mater. Today Commun.*, 2021, **27**, 102286.
10. R. Zhang, B. Xue, Y. Tao, H. Zhao, Z. Zhang, X. Wang, X. Zhou, B. Jiang, Z. Yang, X. Yan and K. Fan, *Adv Mater*, 2022, **34**, e2205324.
11. K. Fan, J. Xi, L. Fan, P. Wang, C. Zhu, Y. Tang, X. Xu, M. Liang, B. Jiang, X. Yan and L. Gao, *Nat Commun*, 2018, **9**, 1440.
12. Y. Z. Hong, Y. H. Jiang, C. S. Li, W. Q. Fan, X. Yan, M. Yan and W. D. Shi, *Appl. Catal. B-Environ.*, 2016, **180**, 663-673.
13. K. Ghorai, A. Panda, M. Bhattacharjee, D. Mandal, A. Hossain, P. Bera, M. M. Seikh and A. Gayen, *Appl. Surf. Sci.*, 2021, **536**, 147604.
14. C. Cui, R. H. Guo, H. Y. Xiao, E. Ren, Q. S. Song, C. Xiang, X. X. Lai, J. W. Lan and S. X. Jiang, *Appl. Surf. Sci.*, 2020, **505**, 144595.
15. P. Chen, F. Z. Sun, W. Wang, F. T. Tan, X. Y. Wang and X. L. Qiao, *J. Alloy. Compd.*, 2020, **834**, 155220.
16. A. Ibarbia, L. Sanchez-Abella, L. Lezama, H. J. Grande and V. Ruiz, *Appl. Surf. Sci.*, 2020, **527**, 146937.